

Proceedings Article

# Validation of spatial selectivity enhancement for magnetic fluid hyperthermia by introducing ferromagnetic cores

K. Sajjamark<sup>a,\*</sup> · H. Lehr<sup>a</sup> · R. Pietig<sup>b</sup> · H. Autz<sup>b</sup> · J. Chacon-Caldera<sup>a</sup> · J. Franke<sup>a</sup>

<sup>a</sup>Bruker BioSpin MRI GmbH, Ettlingen, Germany

<sup>b</sup>Bruker BioSpin GmbH, Rheinstetten, Germany

\*Corresponding author, email: [kulthisa.sajjamark@bruker.com](mailto:kulthisa.sajjamark@bruker.com)

© 2022 Sajjamark *et al.*; licensee Infinite Science Publishing GmbH

This is an Open Access article distributed under the terms of the Creative Commons Attribution License (<http://creativecommons.org/licenses/by/4.0>), which permits unrestricted use, distribution, and reproduction in any medium, provided the original work is properly cited.

## Abstract

Spatial selectivity plays a crucial role in magnetic fluid hyperthermia as it defines the precision of thermal dose localization. We propose to confine the magnetic flux of the selection field coil by introducing ferromagnetic cores with high magnetic permeability. An increased gradient leads to an increased spatial selectivity in both imaging and MPI-assisted magnetic fluid hyperthermia. Thus, this hardware proposal is beneficial for *in situ* theranostic systems and applications. This work validates experimentally the benefits and impacts of magnetic core prototypes to increase the magnetic gradient strength by a factor of 1.3 which suggests a 21% improvement in thermal localization in hyperthermia therapy.

## 1. Introduction

Magnetic Fluid Hyperthermia (MFH) has been shown as a viable cancer therapy [2, 3], which is based on Radio Frequency (RF) magnetic field excitation of biocompatible superparamagnetic nanoparticles. AC magnetization losses within the superparamagnetic nanoparticles lead to energy conversion, which can be leveraged for thermal deposition in a target area [2, 3]. However, the distribution of energy deposition is governed mostly by the nanoparticle distribution and the RF-field amplitude. To provide flexibility and applicability of spatially targeted MFH, the usage of a magnetic field gradient, featuring a field-free-region (FFR), was proposed as spatial encoding mechanism [4, 5]. The same underlying spatial encoding mechanism is known from the novel imaging technology, Magnetic Particle Imaging (MPI). Thus, in both techniques of MPI and MFH, spatial selectivity is dependent on the tracer properties, the selection field gradient slope,

and also RF-field amplitude [6]. Due to the same underlying mechanism, both techniques can be combined into one theranostic system allowing for *in situ* MFH therapy [3, 7] and MPI-based imaging. Moreover, MPI allows also for image-based thermometry [8] which is an asset for non-invasive temperature monitoring during MFH applications. For the Field of View (FOV) in imaging or FOT (Field of Therapy) in MFH, a shift of the FFR can be realized by superimposing quasi-static homogeneous magnetic offset fields [4]. The studies [2, 3, 4] showed, that an increased selection field gradient leads to higher image resolution capabilities and increased spatial selectivity enhancement and thus a minimization of thermal damage in healthy tissue in MFH application.

Since high spatial selectivity is required in MPI-MFH theranostic systems, an increase in magnetic gradient slope was proposed in [1] by adding ferromagnetic cores to the commercially available preclinical MPI system (MPI 25/20 FF, Bruker BioSpin MRI GmbH). According

to Biot-Savart law, adding high permeability core material can significantly confine the magnetic flux [9] in electromagnets.

According to our simulation of this proposed system [1], the field gradient can be increased by a factor of 1.4 by simply adding ferromagnetic cores into the center of selection coils which suggests a 27% improvement in energy localization in MFH therapy. In this work, we evaluate a prototype and present the experimental results.

## II. Material and methods

### II.I. Theranostic system

As basis for a theranostic system, a commercially available preclinical MPI system (MPI 25/20 FF, Bruker BioSpin MRI GmbH) with a cylindrical bore and field-free-point (FFP) gradient topology was used. This MPI scanner consists of 7 channels; Selection Field (SF) coils, 3-axis Focus Field (FF) coils and 3-axis Drive Field (DF) coils. The addition of a 1-axis MFH insert which can generate the maximum RF-field amplitude, so-called MFH-field, of 10mT [10] (Wei *et al.*, Institute of Medical Engineering, University of Lübeck), the preclinical MPI system can be extended to serve as theranostic system and allows for *in situ* MFH.

### II.II. Ferromagnetic core design and simulation

To increase spatial selectivity of the theranostic system, ferromagnetic cores, further developed from [1], were mounted vertically through the center of SF-coil housing (see Figure 1c). Based on the simulation [1], the core dimension was optimized to allow for eased installation and to offer a copper housing to screen the core material from DF-excitation and thus to prevent the generation of harmonic signals in MPI application. The core holder was also designed for the benefits of mechanical fixation and safety aspects during the operation of the magnet system. Based on these boundary conditions, the core configuration was adapted and the core properties and effects onto the system have been simulation with the software ANSYS Maxwell (ANSYS, Inc., Canonsburg, Pennsylvania, U.S.A).

### II.III. Measurement protocol

To compensate the DF-resonance circuitry loading caused by the additional conductive core holder, the tuning capacitors of all resonance circuits (X, Y, and Z) were readjusted using a network analyzer (Agilent Technologies, Inc., Santa Clara, CA). Since the oscillating magnetic field of DF-coils passes directly through the bottom surface of the core holder, eddy current induced

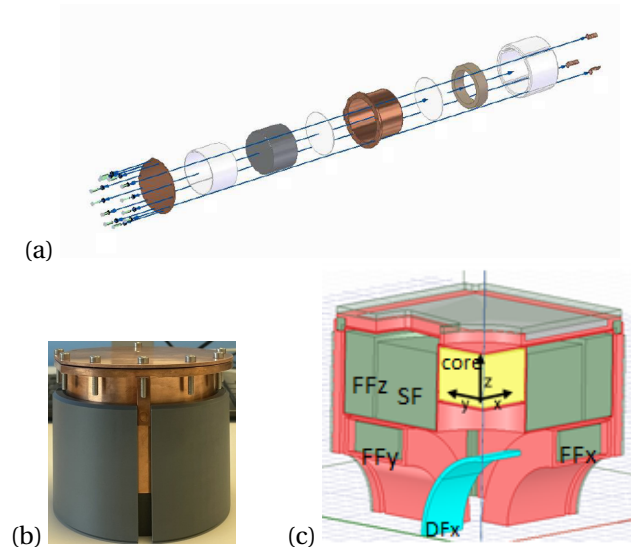


**Figure 1:** Exploded view (a), manufactured core prototype and installation parts (b), and simulated core-inserted scanner (c). In Figure 1a, C is ferromagnetic core, the holder and its cap are shown in components E and A, respectively. Core stabilization is supported by non-magnetic PVC material of D, F and G in z-direction, and B, H, and I in x and y directions.

thermal effects on this component was investigated by a PT100 temperature sensor. In this observation, DF with 14/14/14mT amplitude was operated for 3 hours.

To evaluate the proposed techniques of spatial selectivity enhancement by increased magnetic gradient, the SF-gradient slope was measured in different positions into x, y, and z directions by using gaussmeter (Lake Shore Cryotronics, Inc., Westerville, OH, U.S.A). In this experiment, the current supply was set to provide 160, 200, 330, 400, and 500A, to the SF-coil. The gradient slope and SF-linearity error can be calculated by the measured values of SF-amplitudes and the respective spatial offset [1]. To assess the maximal reachable FOT offsets, the FF-amplitudes were computed by using FF-amplitudes in different positions in x, y, and z directions [1]. Equivalently to SF measurement, the gauss sensor was used for FF-amplitudes measurement.

### II.IV. FOT calculation

For the effect on theranostic therapy, the spatial selectivity of energy deposition on the therapy region can be indicated by the minimum accessible FOT which is calculated by the field amplitude of MFH-field ( $\hat{B}_{MFH}$ ) and SF-gradient slope (G) (1). The FFP offset, which indicates the maximum reachable FOT, is calculated by maximum FF-amplitude ( $\hat{B}_{FF}$ ) and SF-gradient slope (G) (2). Minimum accessible FOT ( $minFOT_i$ ) and maximum accessible FOT ( $maxFFR_i$ ) in direction  $i$  can be calculated

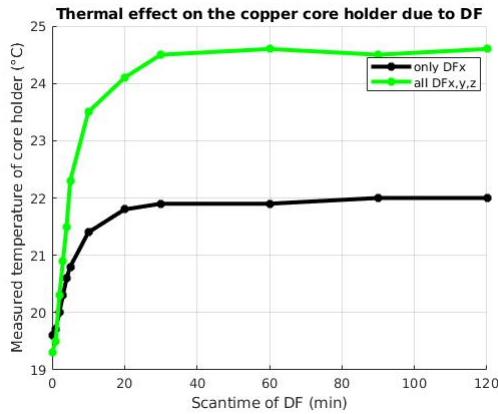


**Figure 2:** Thermal effect induced by eddy current from DF-resonance during the operation of 14mT of DFx, DFy, and DFz.

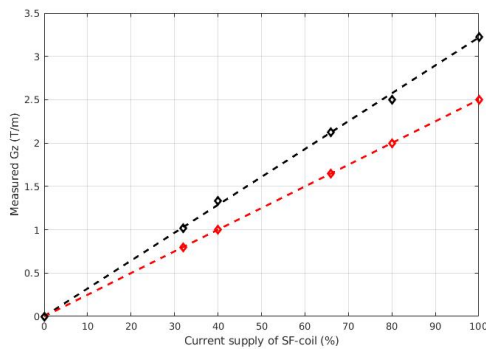


**Figure 3:** Comparison of measured gradient slopes in different levels of SF-currents between the default and proposed systems.

by:

$$\min FOT_i = \frac{2\hat{B}_{MFH_i}}{G_i} \quad (1)$$

and

$$\max FFR_i = \frac{2\hat{B}_{FF_i}}{G_i}, \quad (2)$$

respectively.

## III. Results and discussion

### III.I. Hardware design and installation

The copper-shielded ferromagnetic core was inserted as retrofit to the SF coil housing. The conductive holder and the supporting installation parts (see in Figure 1) were designed to mechanically stabilize the ferromagnetic core during high gradient strength operation of the magnet system. The screw mounting topology was designed to support the yielded electromagnetic force, which was concerned by maximal 600N of the simulated

force generated by SF and FFz coils in vertical direction [1].

### III.II. Measurement results

Regarding to the recent simulation [1], eddy currents, induced by DF, are distributed on the conductive copper material of bottom surface of the holder. Due to this influence, the frequencies were shifted from the optimal response by 2.0 kHz for DFx, 0.8 kHz for DFy, and 0.5 kHz for DFz. The impedance and capacitor were then readjusted to compensate this effect. The copper RF-shielding of the ferromagnetic core was evaluated to be effective by the observation of the DF-induced thermal effect on the holder. By the temperature measurement of this component, the temperature increased during RF excitation and saturated after 30min (see Figure 2).

For the evaluation of our core prototype performance, the result showed that, the proposed configuration of the ferromagnetic core can increase gradient slope in z direction 30% and in x and y directions 27% (see detail in Table 1). The proposed system provides -6.9%, -6.9%, 8.8% of gradient linearity errors for SFx, SFy, and SFz, respectively. The resulting gradient slope values from different levels of SF current can be found in Figure 3. According to Figure 3, the slight deviation from the averaging line might be affected by the calibration of FFP-origin position and the performance of SF-amplifier at higher power. This must be further investigated. The maximum amplitudes of the FFx/FFy/FFz were increased from 17.0/17.0/45.0 mT for the default system to 17.7/17.9/49.4 mT for the system with the magnetic core. Relative homogeneity errors of FFx, FFy, and FFz in x, y, and z-directions, were 34.5%, 33.2%, and 11.3%, respectively. The comparison between measurements with the default and the proposed systems is shown in Table 1.

### III.III. Calculation results

With this increased gradient slope, we can achieve a reduction in the minimal FOTx from 16.0 mm provided by the default system to 12.6 mm by our proposed system, when an additional MFH-coil with the maximal MFH-field amplitude of 10 mT is installed in x-direction. This result corresponds to a 21.25% improvement in the precision of thermal dose localization. Considering the maximum possible FOT, the maximum FFP offsets in x/y/z-directions were reduced from 13.6/13.6/18.0 mm to 11.1/11.2/15.0 mm for the default and proposed systems, respectively.

## IV. Conclusions and outlook

This contribution evaluates experimentally the spatial selectivity enhancement for magnetic fluid hyperthermia

**Table 1:** Comparison of parameter measurements and calculations between the default and the proposed system.

Parameters	Default system		Proposed system	
	Simulation	Experiment	Simulation	Experiment
max $G_x/G_y/G_z$ (T/m)	1.25/1.25/2.5	1.25/1.25/2.50	1.65/1.65/3.3	1.59/1.59/3.23
SF – linearity error (%)	-6.9/-6.9/7.4	-5.3/-5.7/6.3	-6.4/-6.4/7.5	-6.9/-6.9/8.8
Max $A_x/A_y/A_z$ (mT)	18/18/ 44.5	17/17/45.0	18.2/18.2/51.4	17.7/17.9/49.4
FF – relative homogeneity error	32.1/32.8/7	33.7/33.9/6.6	32.5/32.1/12	34.5/33.2/11.3
Calc. max $\Delta x/\Delta y/\Delta z$ (mm)	14.4/14.4/17.8	13.6/13.6/18.0	11.1/11.1/15.6	11.1/11.2/15.02
Calc. min FOT at 10 mT of MFHx (mm)	16.0/0/0	16.0/0/0	12.2/0/0	12.6/0/0

by retrofitted ferromagnetic cores. From the simulation study [1], the proposed modification can increase the performance MFH localization and imaging resolution of the MPI assisted-MFH. Adapted from the simulation [1], the copper holder of the core was additionally designed for harmonic signal prevention and mechanical installation. For this purpose, the dimension of the ferromagnetic core was optimized. The prototype increases the gradient slope with a factor of 1.3, corresponding to approx. 21% increase in precision of thermal dose targeting in MFH with the presence of additional MFH-coil. Moreover, we have also observed the effect of the core prototype on the MPI system. Thermal effect due to DF-excitation are neglectable and permit for safe operation.

To assure the desirable performance of the MPI system, which are magnet saturation and signal quality, further tasks need to be achieved. This includes to assess hysteresis effect of the magnetic core material on SF and FF fields. Furthermore, the effect on signal spectrum and the long-term stability of the system must be evaluated. Also, the benefits for imaging with the proposed MPI system need to be performed to prove an increased spatial resolution in imaging.

## Acknowledgments

Acknowledgement of research funding: The work is a part of “Functional Magneto-Therapy” project which is funded by the German Federal Ministry of Education and Research (BMBF, grant number 13GW0230C).

## Author’s statement

K. Sajjamark, H. Lehr, J. Chacon Caldera, and J. Franke are the employees of Bruker BioSpin MRI GmbH, whereas

R. Pietig, H. Autz are the employees of Bruker BioSpin GmbH.

## References

- [1] K. Sajjamark, H. Lehr, R. Pietig, N. Volker, and J. Franke. Spatial selectivity enhancement in magnetic fluid hyperthermia by magnetic flux confinement, *International Journal on MPI*, vol.6(2), 2020.
- [2] Z. W. Tay, P. Chandrasekharan, A. Chiu-Lam, D. W. Hensley, R. Dhavalikar, X. Y. Zhou, E. Y. Yu, P.W. Goodwill, B. Zheng, C. Rinaldi, and S. M. Conolly. Magnetic Particle Imaging-Guided Heating in Vivo Using Gradient Fields for Arbitrary Localization of Magnetic Hyperthermia Therapy. *ACS Nano*, 12(4):3699–3713, 2018.
- [3] K. Murase, M. Aoki, N. Banura, K. Nishimoto, A. Mimura, T. Kuboyabu, and I. Yabata. Usefulness of Magnetic Particle Imaging for Predicting the Therapeutic Effect of Magnetic Hyperthermia. *Open Journal of Medical Imaging*, 05(02):85–99, 2015
- [4] J. Rahmer, J. Weizenecker, B. Gleich, and J. Borgert. Signal encoding in magnetic particle imaging: properties of the system function, *BMC Medical Imaging*, 9:4, 2009.
- [5] B. Gleich and J. Weizenecker. Tomographic imaging using the nonlinear response of magnetic particles, *Nature*, 435(7046):1214–1217, 2005.
- [6] Weber, A., et al. "Resolution improvement by decreasing the drive field amplitude." 2015 5th International Workshop on Magnetic Particle Imaging (IWMPi). IEEE, 2015.
- [7] A. Malhotra, A. von Gladiss, A. Behrends, T. Friedrich, A. Neumann, T. M. Buzug, and K. Lüdtke-Buzug. Tracking the Growth of Superparamagnetic Nanoparticles with an In-Situ Magnetic Particle Spectrometer (INSPECT), *Scientific Reports*, 9(1):10538, 2019.
- [8] C. Stehning, B. Gleich, and J. Rahmer. Simultaneous magnetic particle imaging (MPI) and temperature mapping using multicolor MPI, *International Journal on Magnetic Particle Imaging*, 2(2), 2016.
- [9] A. Moses, A. Moses, P. Anderson, and K. Jenkins. *Electrical Steels Fundamentals and basic concepts*, 1st ed. vol. 1, IET publisher, NJ, 2019, pp. 141-170.
- [10] H. Wei, A. Behrends, T. Friedrich, and T. Buzug. A heating coil insert for a preclinical MPI scanner, *International Journal on MPI*, vol.6(2), 2020.